ISSN 1392-2114 ULTRAGARSAS, Nr.2(39). 2001.

Visualisation of high frequency structural micro vibrations under static thermal loads

M. Ragulskis[1)], L. Ragulskis[2)] , J. Ragulskiene[3)]

1) Department of Software Engineering, Kaunas University of Technology

Studentų st. 50, LT-3031, Kaunas, Lithuania

2)University of Vytautas the Great,

Vileikos 8, Kaunas, Lithuania

3)Department of Engineering, Lithuanian University of Agriculture

Noreikiskes, Kaunas, Lithuania

Introduction

The determination of the interference bands of the plate as a structural element performing the harmonic motion according to the eigenmode by taking into account the statical thermal deflection is presented.

Numerical determination of the interference bands

Let the planes *A*, *B* and *C* be defined in the 3 dimensional space (Figure 1). Let the triangle defined by points 1, 2 and 3 be located in plane A. This triangle is interpreted as an elementary body surface unit meshed using the Finite Element Method [7]. Let the coordinates of the point $\boldsymbol{r}_1$ define the observation point. Let the projection plane be defined by points $\boldsymbol{r}_2$, $\boldsymbol{r}_3$ and $\boldsymbol{r}_4$. Let $\boldsymbol{r}_5$ be the vector from the point of the structure to the isophase cross section of the laser beam in the direction of the beam.

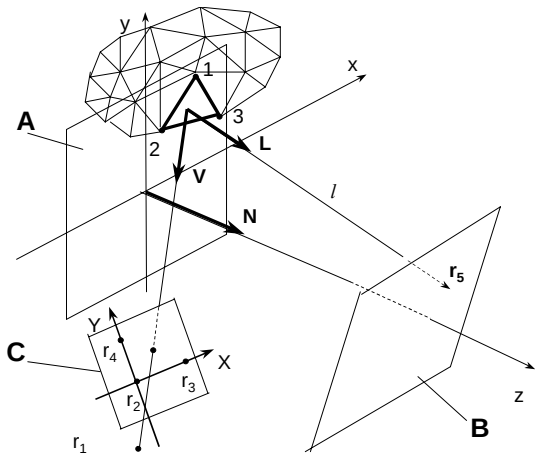

Fig. 1. **Determination of the intensity of the surface: A – plane of the structure, B – cross section of the laser beam, C – projection plane**

Assuming that $\boldsymbol{r}_1$ is the observation point, $\boldsymbol{r}_2$ is the frame point and $\boldsymbol{r}_3$, $\boldsymbol{r}_4$ are points (1,0) and (0,1) of the projection plane, (x,y,z) – point on the projection plane, the equations can be rearranged in a matrix form:

$$\begin{bmatrix} x_2 & x_3 & x_4 & -x_1 & -x \\ y_2 & y_3 & y_4 & -y_1 & -y \\ z_2 & z_3 & z_4 & -z_1 & -z \\ 1 & 1 & 1 & 0 & 0 \\ 0 & 0 & 0 & 1 & 1 \end{bmatrix} \begin{Bmatrix} L_1 \\ L_2 \\ L_3 \\ L_4 \\ L_5 \end{Bmatrix} = \begin{Bmatrix} 0 \\ 0 \\ 0 \\ 1 \\ 1 \end{Bmatrix}. \tag{1}$$

Then the co-ordinates of the point in the projection plane may be found:

$$\begin{aligned} X &= (\tilde{x} - x_2)(x_3 - x_2) + (\tilde{y} - y_2)(y_3 - y_2) + \\ &+ (\tilde{z} - z_2)(z_3 - z_2) \\ Y &= (\tilde{x} - x_2)(x_4 - x_2) + (\tilde{y} - y_2)(y_4 - y_2) + \\ &+ (\tilde{z} - z_2)(z_4 - z_2) \end{aligned} \tag{2}$$

where

$$\begin{aligned} \tilde{x} &= L_4 x_1 + L_5 x \\ \tilde{y} &= L_4 y_1 + L_5 y \\ \tilde{z} &= L_4 z_1 + L_5 z \end{aligned} . \tag{3}$$

The spatial co-ordinates (x,y,z) of the point in the projection plane can be determined from:

$$\begin{bmatrix} x_3 - x_2 & y_3 - y_2 & z_3 - z_2 \\ x_4 - x_2 & y_4 - y_2 & z_4 - z_2 \\ x_0 & y_0 & z_0 \end{bmatrix} \begin{Bmatrix} x \\ y \\ z \end{Bmatrix} = \begin{Bmatrix} X + x_2(x_3 - x_2) + y_2(y_3 - y_2) + z_2(z_3 - z_2) \\ Y + x_2(x_4 - x_2) + y_2(y_4 - y_2) + z_2(z_4 - z_2) \\ x_2 x_0 + y_2 y_0 + z_2 z_0 \end{Bmatrix} \tag{4}$$

where

$$\begin{aligned} x_0 &= (y_3 - y_2)(z_4 - z_2) - (z_3 - z_2)(y_4 - y_2) \\ y_0 &= (z_3 - z_2)(x_4 - x_2) - (x_3 - x_2)(z_4 - z_2) \\ z_0 &= (x_3 - x_2)(y_4 - y_2) - (y_3 - y_2)(x_4 - x_2) \end{aligned} , \tag{5}$$

and (X,Y) – the coordinates of a point in the projection plane. This follows from:

$$\begin{aligned}&(x-x_2)(x_3-x_2)+(y-y_2)(y_3-y_2)+\\&+(z-z_2)(z_3-z_2)=X\\&(x-x_2)(x_4-x_2)+(y-y_2)(y_4-y_2)+\\&+(z-z_2)(z_4-z_2)=Y\\&(x-x_2)x_0+(y-y_2)y_0+(z-z_2)z_0=0\end{aligned} \quad (6)$$

Assuming there are i=1,...,n rows and j=1,...,m columns of pixels the calculations are performed for:

$$\begin{aligned}X&=X_{\min}+(j-1)\left(X_{\max}-X_{\min}\right)/(m-1)\\Y&=Y_{\max}-(i-1)\left(Y_{\max}-Y_{\min}\right)/(n-1)\end{aligned}. \quad (7)$$

Every Lagrange quadratic rectangular finite element [7] is subdivided into eight linear triangles. As the structure is located in the plane z = 0 in the status of equilibrium, and assuming $(\hat{x}_i, \hat{y}_i)$, i = 1,2,3 as nodal co-ordinates of a linear triangle element, the following relationship is found:

$$\begin{bmatrix}\hat{x}_1 & \hat{x}_2 & \hat{x}_3 & -x_1 & -x\\ \hat{y}_1 & \hat{y}_2 & \hat{y}_3 & -y_1 & -y\\ 0 & 0 & 0 & -z_1 & -z\\ 1 & 1 & 1 & 0 & 0\\ 0 & 0 & 0 & 1 & 1\end{bmatrix}\begin{Bmatrix}L_1\\L_2\\L_3\\L_4\\L_5\end{Bmatrix}=\begin{Bmatrix}0\\0\\0\\1\\1\end{Bmatrix} \quad (8)$$

The local co-ordinates of the nodal points of the Lagrange finite element are (–1,–1), (0,–1), (1,–1), (–1,0), (0,0), (1,0), (–1,1), (0,1), (1,1). That enables finding approximate local co-ordinates of an element by interpolation from the local co-ordinates of the nodes of a linear triangle. Then the shape functions of the element can be easily calculated. Besides, the normal vector $\boldsymbol{N}$ coincides with the unit vector of the z axis.

Thus the approximate co-ordinates x and y of the intersection point are obtained by interpolation, and the point on the surface is given as a vector

$$\boldsymbol{r}=\begin{Bmatrix}x\\y\\0\end{Bmatrix} \quad (9)$$

It is assumed that the laser rays are coherent and parallel to each other.

The vector from $\boldsymbol{r}$ to the isophase cross section of the laser beam in the direction of the beam is $\boldsymbol{r}_5$. The length of this vector is the distance between the light source and the point of the surface, the corresponding unit vector is the direction to the light source.

Further, the relationship between the direction to the light source and the direction of reflection can be described by the known equation [2]. In our notation $\boldsymbol{R}$ is the direction of reflection, $\boldsymbol{L}$ – the direction to the light source, $\boldsymbol{N}$ – the normal vector to the structure plane (Fig. 1).

As it is assumed that the surface of the plate is statically deflected from the position of equilibrium and at the same time performs harmonic oscillations of an appropriate eigenform, the intensity is calculated as:

$$I=\left(k_d(N\cdot L)+k_s(V\cdot R)^n\right)\cdot\overline{\cdot\cos^2\left(2\pi\left(l-(u_1\cdot L)-(u_2\cdot L)\sin\omega t\right)/\lambda\right)} \quad (10)$$

where u_1 is the statical deflection and u_2 is the amplitude of harmonic oscillations, k_d is the product of the source intensity and the diffuse reflection coefficient, k_s – the product of the source intensity and the specular reflection coefficient, n is a coefficient describing the smoothness of the surface, V is the direction to the viewer, l is the distance between the light source and the point on the surface, λ is the laser wavelength, the top line denotes averaging by time. When $(N\cdot L)$ is negative it is assumed to be equal to 0, when $(V\cdot R)$ is negative it is assumed 0 also.

Numerical averaging of (10) is performed using at least 64 intermediate state positions of the surface during one cycle of eigenwavelength. The selection of the number of intermediate states is based on the number of intensity levels which are used for the construction of the digital image. Numerical experiments prove that quadruple of the number intensity level is sufficient for production of high quality images. The averaged term takes the form:

$$\overline{\cos^2\left(2\pi\left(l-(u_1\cdot L)-(u_2\cdot L)\sin\omega t\right)/\lambda\right)}=\frac{1}{n}\sum_{j=1}^{n}\cos^2\left(\frac{2\pi}{\lambda}\begin{pmatrix}l-(u_1\cdot L)-\\-(u_2\cdot L)\sin\left(2\pi(j-1)/n\right)\end{pmatrix}\right) \quad (11)$$

The nodal variables are w, Θ_x, Θ_y (it is assumed that $v = -z\Theta_x$, $u = z\Theta_y$). The stiffness and mass matrices are:

$$K=\iint\left(B^TDB+\overline{B}^T\overline{D}\,\overline{B}\right)dxdy$$

$$D=\frac{h^3}{12}\begin{bmatrix}\frac{E}{1-\nu^2} & \frac{E\nu}{1-\nu^2} & 0\\ \frac{E\nu}{1-\nu^2} & \frac{E}{1-\nu^2} & 0\\ 0 & 0 & \frac{E}{2(1+\nu)}\end{bmatrix}$$

$$\overline{D}=\frac{Eh}{2(1+\nu)1.2}\begin{bmatrix}1 & 0\\ 0 & 1\end{bmatrix}$$

$$B=\begin{bmatrix}0 & 0 & \frac{\partial N_1}{\partial x} & \vdots & \\ 0 & -\frac{\partial N_1}{\partial y} & 0 & \vdots & \cdots\\ 0 & -\frac{\partial N_1}{\partial x} & \frac{\partial N_1}{\partial y} & \vdots & \end{bmatrix}$$

$$\overline{B}=\begin{bmatrix}\frac{\partial N_1}{\partial y} & -N_1 & 0 & \vdots & \cdots\\ \frac{\partial N_1}{\partial x} & 0 & N_1 & \vdots & \cdots\end{bmatrix}$$

$$M = \iint [N]^T \begin{bmatrix} \rho h & 0 & 0 \\ 0 & \frac{\rho h^3}{12} & 0 \\ 0 & 0 & \frac{\rho h^3}{12} \end{bmatrix} [N] dxdy$$

$$[N] = \begin{bmatrix} N_1 & 0 & 0 & \vdots & \\ 0 & N_1 & 0 & \vdots & \cdots \\ 0 & 0 & N_1 & \vdots & \end{bmatrix} \quad (12)$$

where E – the modulus of elasticity, ν – the Poissons ratio, h – the thickness of the plate, ρ – density of the material of the plate.

The thermal load vector is assumed to take the following form [8]:

$$F = \iint B^T D \begin{Bmatrix} \alpha T \\ \alpha T \\ 0 \end{Bmatrix} dxdy \quad (13)$$

here α – the coefficient of thermal expansion, T – the increase in temperature between the points separated by a unit of length in the z direction. T can be determined from the solution of the one-dimensional static heat transfer equation in the direction of the z axis.

The differential equation of motion is:

$$M\ddot{\delta} + K\delta = F_1 + F_2 \sin \omega t \quad (14)$$

where δ – the vector of nodal displacements.

The steady state solution may be assumed as: $\delta = \delta_1 + \delta_2 \sin \omega t$. That produces: $(K - \omega^2 M)\ \delta_2 \sin \omega t + K\delta_1 = F_1 + F_2 \sin \omega t$. Finally, this leads to:

$$K\delta_1 = F_1 \quad (17)$$

$$(K - \omega^2 M)\ \delta_2 = F_2 \quad (18)$$

In our case it is assumed that the given constant thermal loading produces a statical displacement and that the steady state dynamic loading produces harmonic motion according to the given eigenmode.

Numerical investigations

The numerical holographic interferograms of the micro-vibrations of the plate are presented in Fig. 2 – 5.

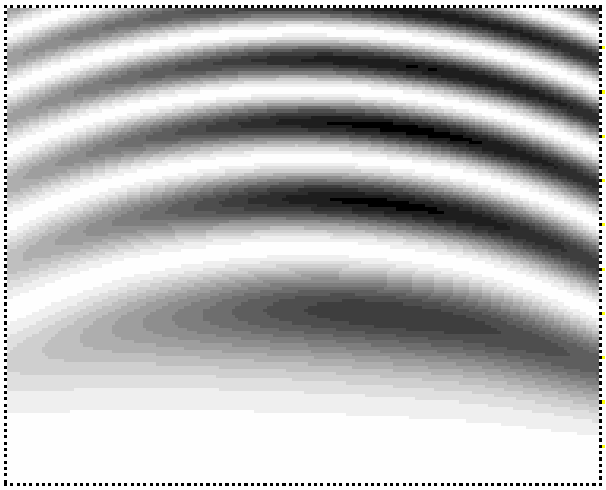

Fig. 2. **The hologarphic interferogram of the static deflection caused by thermal load**

The analysed object was an elastic plate with motionlessly clamped lower side edge. The mathematical model of the system was developed based on the previous relationships taking into account the static thermal load. The holographic interferogram of the static deflection from the thermal load was found (Fig. 2). First eigenmodes were calculated using subspace iteration method [7].

The holographic interferogram of the third eigenmode is presented in Fig. 3. It is evident that with the increase of the amplitude of vibrations, the sharpness of the image decreases. That fully corresponds to the known theoretical analysis of the holographic images [9].

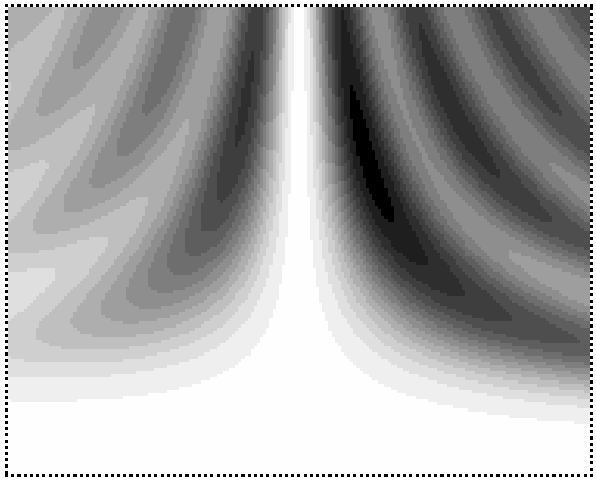

Fig. 3. **The time average holographic interferogram of the third eigenmode**

The method of two exposures used for statical holograms was generalised on the basis of previous investigations in [3–6] for the purpose of better visualisation of relatively high amplitudes of micro vibrations. Four exposure method enables the averaging of the sequential states (the equilibrium, the maximum displacement according to the eigenmode, again the equilibrium, the maximum displacement according to the eigenmode in the opposite direction). The holographic image of the same eigenmode using four exposition method is presented in Fig. 4. It is seen that this method produces an image of better sharpness, moreover the method requires a smaller amount of calculations.

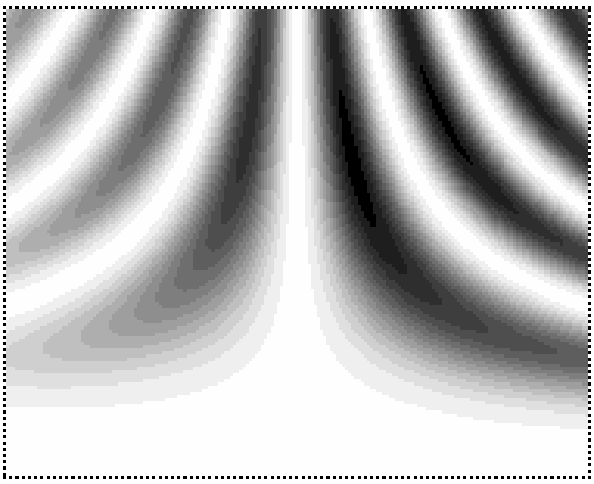

Fig. 4. **The four exposure holographic interferogram of the third eigenmode**

The time averating procedure used for micro vibration analysis [9] leads to the analytical relationships involving Bessel functions. Eq. 10 – 11 generalise the time averaging procedure for vibration analysis for the problems when vibrations take place with respect to the statically deflected state. That involves more complicated analytical relationships which lead to shifted argument Bessel functions. Further analytical investigations of these functions encounter substantial mathematical difficulties and run out of scope of analysed typical problems presented in [9]. Nevertheless, numerical averaging procedures enable to overcome those difficulties.

Such problems can be found in such experimental arrangements when heating appliances are not properly allocated in the laboratory, or the friction generated heat (e.g. ultrasonic motor contacting surfaces) distorts homogeneous temperature distribution of the experimental set-up.

The holographic interferogram of the plate vibrating according to the third eigenmode and simultaneously exposed to static external thermal load is presented in Fig. 5.

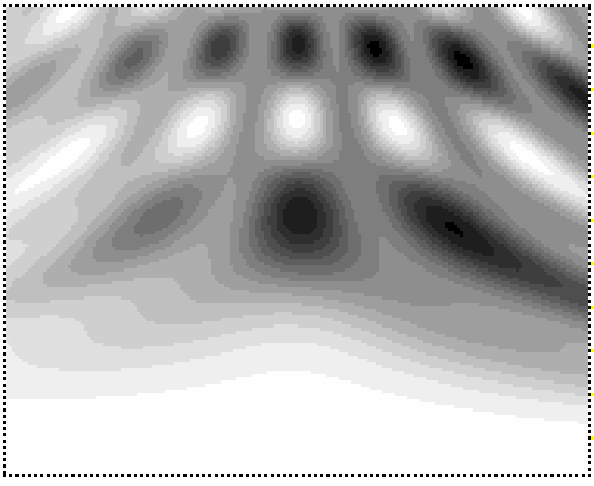

Fig. 5. **The holographic interferogram of the third eigenmode with the thermal static load**

It should be noted that in all presented interferograms the laser beam is not perpendicular to the surface of the analysed plate in equilibrium state. The importance of the ability of generating the holographic interferograms with the incident beam from various directions of lightning lies in the necessity to better interpret the amplitudes of the vibrations of the structure and was indicated in [2].

Conclusions

The holographic interferogram generation method is developed for the statically shifted steady state harmonic micro vibrations. The influence of external thermal load is integrated in the model of the analysed system. That enables more qualitative assessment of real holographic images of the dynamics of structures under more complicated environmental conditions.

References

1. **Palevičius A., Ragulskis M., Palevičius R.** Wave mechanical systems (theory, holographic interferometry). ISBN 9986-461-23-5. Kaunas: Caritas, 1997. P 149.
2. **Palevičius A.** General theory for quantative evaluation of three-dimensional vibrations from time-average holographic interferograms. Ultrasound. Kaunas: Technologija. 2001. No 1(38). P. 7-17.
3. **Ilgakojis P., Ragulskienė J., Palevičius A., Ragulskis M.** Parametric optimization of the vibration clasification system. - The 70th Shock &Vibration Symposium: Sandia National Laboratories, SAVIAC, November 15-19, Albuquerque, New Mexico, 1999.
4. **Ragulskis M., Palevičius A., Ostaševičius V.** Investigation of the dynamic behavior of transmission Coupling's Half Clutch. - SAE 2000 WORLD CONGRESS, March 6 – 9, Cobo center, Detroit, Michigan, USA. 2000. No.2000-01-0839. P.5.
5. **Palevičius A., Tomasini E. P., Ragulskis M.** Vibromotors optimization using laser holographic interferometry. – Proc. of the 17th Int. Modal analysis conf., organized by Society for Experimental mechanics, February 8-11, 1999, Florida. P.1012-1015.
6. **Palevičius R., Ragulskis M., Palevičius A.** A system for holographic interferometry experimental data processing. – Information technology and control. Kaunas: Technologija, 1999. No 4(13). P.47-51.
7. **Bathe K. J.** Finite element procedures in engineering analysis. – New Jersey: Prentice-Hall, 1982. P. 735.
8. **Rao S. S.** The finite element method in engineering. – Oxford: Pergamon Press. 1982. P. 626.
9. **Vest C.M.** Holographic interferometry. Wiley, New York, 1979.

M. Ragulskis, L. Ragulskis, J. Ragulskienė

Aukšto dažnio konstrukcinių mikrovirpesių vizualizacija esant statinėms terminėms apkrovoms

Reziume

Išvystytas holografinių interferogramų generavimo metodas statiškai pastumtiems nusistovėjusiems harmoniniams mikrovirpesiams. Išorinės terminės apkrovos įtaka yra integruota į analizuojamos sistemos modelį. Tai įgalina kokybiškiau įvertinti realius konstrukcijų dinamikos holografinius vaizdus esant sudėtigesnėms supančios aplinkos sąlygoms.

Pateikta spaudai 2001 04 23

DOI: 10.5755/j01.u.39.2.8052